
This is an electronic reprint of the original article.
This reprint may differ from the original in pagination and typographic detail.

Sheikh, Muhammad Usman; Ruttik, Kalle; Jäntti, Riku; Hämäläinen, Jyri

Analysis of radio propagation with different antenna solutions at sub-THz band in an indoor (tee-junction) environment using ray tracing simulations

Published in:
Telecommunication Systems

DOI:
[10.1007/s11235-025-01360-5](https://doi.org/10.1007/s11235-025-01360-5)

Published: 01/12/2025

Document Version
Publisher's PDF, also known as Version of record

Published under the following license:
CC BY

Please cite the original version:
Sheikh, M. U., Ruttik, K., Jäntti, R., & Hämäläinen, J. (2025). Analysis of radio propagation with different antenna solutions at sub-THz band in an indoor (tee-junction) environment using ray tracing simulations. *Telecommunication Systems*, 88(4), Article 128. <https://doi.org/10.1007/s11235-025-01360-5>

This material is protected by copyright and other intellectual property rights, and duplication or sale of all or part of any of the repository collections is not permitted, except that material may be duplicated by you for your research use or educational purposes in electronic or print form. You must obtain permission for any other use. Electronic or print copies may not be offered, whether for sale or otherwise to anyone who is not an authorised user.



Analysis of radio propagation with different antenna solutions at sub-THz band in an indoor (tee-junction) environment using ray tracing simulations

Muhammad Usman Sheikh¹ · Kalle Ruttik¹ · Riku Jäntti¹ · Jyri Hämäläinen¹

Received: 12 July 2024 / Accepted: 28 September 2025
© The Author(s) 2025

Abstract

The terahertz (THz) and sub-terahertz (Sub-THz) bands are prime candidates for the sixth-generation (6G) wireless communication system, especially for indoor scenarios. In these frequency ranges, key challenges include high propagation loss, substantial molecular absorption, weak diffraction, and the constraint of restricted transmit power despite broad bandwidths. The considerable bandwidth available at the sub-THz band makes it an appealing and enticing option. However, the challenges mentioned earlier pose difficulties in deploying sub-THz systems. Therefore, it is imperative to conduct thorough radio propagation studies to assess the feasibility and deployment possibilities of communication systems operating in the sub-THz frequency range. One of the targets of this work is to precisely identify channel variations at the sub-THz band, and then compare the performance of different antenna solutions at the receiving end in coping with those variations. In this regard, we carried out a comprehensive campaign of ray tracing simulations considering both line-of-sight (LOS) and non-LOS (NLOS) conditions in an indoor scenario. Our internally developed 3D ray tracing tool was calibrated and validated through measurements before being employed for this research work. Ray tracing techniques can deliver results with high accuracy and precision; however, they have substantial computational complexity, and that restricts the scalability of simulations. In this research work, a realistic scenario of the user walking through the tee-junction of the corridor is considered, while being served by the transmitter located in the other wing of the corridor. This article mainly evaluates the coverage aspects of the indoor network employing different antenna solutions at the receiver, i.e., a single fixed beam antenna, an ideal adaptive antenna with beam steering capability, and a switched beam antenna (SBA), at a sub-THz frequency of 100 GHz. We evaluate the impact of different beam pointing error for adaptive antennas and the number of overlapping beams for SBAs, on the received signal power level. The acquired results reveal that in the case of an ideal adaptive antenna, an almost 20 dB signal power is lost while migrating from 3.5 GHz to 26.5 GHz, followed by an additional 14.5 dB loss when transiting from 26.5 GHz to 100 GHz. The findings presented in this article establish a foundation for future investigations of wireless systems in the sub-THz frequency range.

Keywords Simulations · Ray tracing · Sub-THz · Indoor · Switched beam antenna · Smart antenna · Adaptive antenna

✉ Muhammad Usman Sheikh
muhammad.sheikh@aalto.fi

Kalle Ruttik
kalle.ruttik@aalto.fi

Riku Jäntti
riku.jantti@aalto.fi

Jyri Hämäläinen
jyri.hamalainen@aalto.fi

¹ Department of Communications and Networking, Aalto University, 02150 Espoo, Finland

1 Introduction

The world of wireless technology is witnessing continuous growth in the demand for high-data-rate applications. The ample amount of un-utilized spectrum available at sub-THz frequencies, i.e., between 100 GHz and 300 GHz has got the attention of researchers from academia as well as the industry, and is considered a potential solution for data-intensive applications with high data rate requirements [1, 2]. Large available bandwidth at the sub-THz band along with the potential of building an antenna array with a large number of antenna elements, offers the possibility to provide extremely

high data rates. Thanks to the small wavelength at the sub-THz band, it is possible to integrate a large number of antenna elements in a compact space. While a sub-THz communication offers an opportunity, several challenges, including high propagation, atmospheric absorption, and penetration loss, are also associated with sub-THz communication [3]. Due to the sufficiently large wavelength at the sub-6GHz band, antenna arrays were mainly targeted at the TX end. However, to provide good link budget margins at the sub-THz band, large antenna arrays can be deployed at both the TX and RX ends.

Antenna arrays with a large number of elements provide high gain with a narrow beam, which may help in mitigating the propagation issue of large pathloss at the sub-THz band. However, high-gain antennas with narrow beams have a clear limitation of angular coverage. The issue of coverage can be resolved either by using active adaptive antennas with beam steering capability or by employing a switched beam antenna (SBA), which belongs to the family of smart antennas [4]. It should be noted that precise beam steering is a complex process and requires advanced digital signal processing. Whereas, the design of SBA is less complex and has a low cost compared with antennas with digital beamforming capability [4]. On the other hand, SBA effectively improves the coverage and reduces the interference in the system compared with a conventional single wide beam antenna. There is a trade-off between performance and simplicity, and in general, the digital beam forming offers enhanced flexibility and better performance compared with SBA, at the expense of increased complexity and cost [5].

To develop and design a reliable communication link at the sub-THz band in an indoor environment, the radio propagation aspects of sub-THz communication should be studied. Deep knowledge of sub-THz radio channels from realistic deployment scenarios can be obtained through sophisticated ray tracing (RT) simulations. Ray tracing falls under the category of a deterministic channel model for radio propagation and requires detailed map information for computation. Single-frequency ray tracing simulations have been widely used for wireless systems in both indoor and outdoor environments [6, 7]. Ray tracing techniques can deliver results with high accuracy and precision; however, they have substantial computational complexity, and that restricts the scalability of simulations.

The characteristics of radio propagation at a mmWave frequencies are already significantly different compared with the sub-6GHz band. Now, there is a need to explore the opportunities and challenges posed by the sub-THz band for indoor scenarios. The ultimate application of a sub-THz communication system highly depends on the usage scenario. The primary focus of the sub-THz communication has been on short-range indoor scenarios [1–3, 8–11], and we have also considered the tee-junction of the indoor University corridor

environment for this study. Prior to this study, to properly assess the potential and limitations of sub-THz communications at 100 GHz band, the primary knowledge of propagation environment and channel characteristics was obtained and validated through measurements and ray tracing simulations [12, 13]. Whereas, in this work, the coverage aspects of the indoor network employing different antenna solutions at the receiver, i.e., a single fixed beam antenna, an ideal adaptive antenna with beam steering capability, and a switched beam antenna, at the sub-THz frequency of 100 GHz are analyzed. The impact of different beam pointing errors for adaptive antennas, and the number of overlapping beams for SBAs is evaluated by 3D ray tracing simulations in a common indoor environment, i.e., a tee-junction of a University corridor.

2 Background theory

2.1 Sub-THz radio propagation

Due to the large available spectrum, the sub-THz frequency band, i.e., frequencies between 100 GHz and 300 GHz, is considered a key facilitator for future communication systems, e.g., beyond 5G (B5G), and sixth generation (6G) of wireless networks [1, 2, 11]. Generally, circuits and antennas designed for sub-THz frequency bands are compact in size due to the shorter wavelengths associated with this range. The sub-THz frequency band offers substantially large contiguous bandwidth, which helps in providing high peak data rate and low latency in data transfer. On the other side, certain challenges are associated with sub-THz communication, i.e., high free-space path loss and atmospheric absorption compared with sub-6GHz and millimeter wave (mmWave) frequency bands [1], and high losses for reflection and diffraction [2]. Additionally, due to the limitation of the maximum allowed transmission power and large system bandwidth, it is difficult to provide high transmit power over the bandwidth, it limits the coverage of the sub-THz communication system to a small area. To address these issues, antennas with high gain and narrow half-power beamwidth (HPBW) are used [3]. Generally, systems operating at sub-THz are supposed to be used only at hot spots and capacity-demanding zones. Nevertheless, there are various applications of THz communication, including backhaul/fronthaul link [8], in data centers as a replacement of cables, immersive services like augmented and virtual reality with stringent data rate and latency requirement [2], communication inside the train and aircraft [8], etc.

2.2 Smart antennas

Generally, smart antenna technologies are categorized into adaptive spatial digital processing (beam steering) technol-

ogy and switched-beam antenna technology. Active adaptive antennas with beam steering capability emerge as strong contenders for inclusion in the next-generation wireless communication systems [14]. Beam steering can be achieved by several techniques, such as employing integrated lens antennas and using adaptive or phase array antennas. Fortunately, the small wavelength at the sub-THz band makes it possible to employ a large-scale antenna to cope with the issue of high propagation losses at higher frequencies using beam forming and beam steering with narrow beam [5, 15]. However, transmission with a narrow beam poses the challenge of finding the right beam-pointing direction and precise beam tracking in the case of a mobile receiver. Here, the beam pointing error or beam estimation error is defined as the angular difference between the intended beam direction and the actual beam direction in the azimuth plane. The existence of a beam estimation error at the receiver end tends to steer the beam in an unwanted direction and has a direct impact on the performance and quality of the communication link. The presence of beam estimation error not only leads to the reduction of received power, but may inadvertently also pick up the interference from other sources or cause interference to others. Therefore, it is crucial to analyze the impact of beam estimation error on sub-THz communication.

Beamforming and beam steering require a large number of antenna elements, which results in a more bulky and cumbersome antenna with high losses [16]. Due to its ease of implementation, the switched beam antenna technology is widely utilized in current communication systems. SBA is well-known for suppressing multi-user interference, which helps in increasing the overall capacity of the system [17]. SBA provides concentrated energy in the intended direction with beam-switching capability and can significantly improve the quality of the communication link by minimizing interference without increasing the transmit power [18]. The high-gain SBA can be designed with a monopole, quasi-Yagi dipole, and lens array [17]. The polarization attributes of the antenna elements can be used to design the SBA with anti-interference capability. Several designs of SBA at millimeter-wave (mmWave) bands have already been proposed in literature, which include the use of Butler matrices [19–21], and utilization of linearly polarized transmit arrays [22]. Similarly, at sub-6GHz band, the design of a simple switched beam antenna for LTE in small cell application, and a wideband SBA for full 360° coverage is proposed at reference [23] and [24], respectively.

2.3 Ray tracing

The key functionality of the ray tracing model is to determine the propagation paths from the transmitter point to the receiver point. In the case of free space propagation, there is only a direct path. However, in a real-world envi-

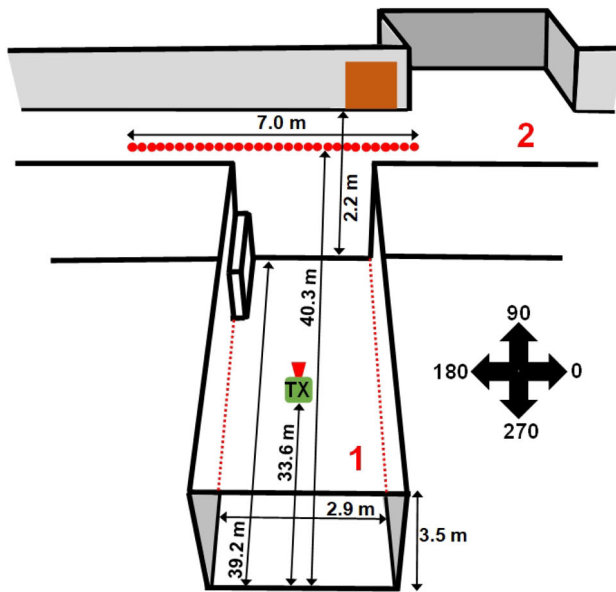
ronment, there exist multiple propagation paths between a source point and a field point through reflections, diffractions, a combination of reflections and diffractions, scattering, and penetration [25]. There are different ways by which these paths can be determined, and it has been a hot research area for researchers. In literature, RT algorithms are mainly classified into three main categories, i.e., image theory (IT) method [7], ray launching or shoot and bouncing ray (SBR) method [26, 27], and hybrid method. Finding ray paths with multiple reflections through the image theory method is a recursive process and requires high computational power for complex environments with a large number of reflecting surfaces. Whereas, in the case of the SBR method, a certain number of uniformly distributed rays are launched from the source point, and these rays continue to propagate with a defined number of reflections and diffractions. The SBR method involves the reception test, and each ray goes through this reception test at the receiving point. While the SBR method requires relatively less computation, it may not yield the same level of precision in determining ray trajectories as the image method. The hybrid approach combines the benefits of SBR, i.e., less computational processing, with those of the IT method, i.e., precise ray path trajectories [28]. Different methods have been proposed to speed up the computation of ray trajectories [25]. In this work, the authors have developed an in-house built ray tracing tool based on image theory. An in-house built RT was calibrated and validated through an extensive measurement campaign at the sub-THz band in an indoor corridor environment for both LOS and NLOS positions [12, 13]. The RT tool provides different properties of each ray, including path number, the distance of the ray path, reflection and diffraction order, E-field, H-field, power, phase, the direction of departure (DoD), and direction of arrival (DoA) in the azimuth plane, angle of departure (AoD), and angle of arrival (AoA) in the elevation plane, etc. These properties of ray paths can be used to compute the delay spread and power delay profile of the channel. However, in this paper, the analysis was limited to received power only.

3 Simulation setup and methodology

For the study purpose of this research work, an in-house built three-dimensional RT tool in MATLAB is employed to perform a series of accurate ray tracing simulations. The RT tool considers an isotropic radiating antenna at the TX and RX ends. Considering the geometry of the environment and other objects, our RT provides details of available ray paths with a predefined number of specular reflections and diffractions. It is important to highlight here that there is no requirement to incorporate directive antennas in the ray tracing simulation process, as they can be considered during the post-processing



(a)



(b)

Fig. 1 The environment under consideration, (a) Actual University corridor, and (b) 3D model of a corridor's tee-junction with TX and RX positions

phase to assess different antenna patterns or beamforming strategies. Our ray tracing tool can capture LOS paths, other paths solely with a defined number of reflections and diffractions, paths with combinations of reflections and diffractions, and paths with diffuse scattering off the walls. Apart from these, the in-house built RT simulation tool detects reflected paths from the ground and ceiling of the environment. However, penetrated paths through the walls of the corridor are

excluded. Here, we have accounted for ray paths involving different combinations, including a maximum of two reflections and one diffraction, along with diffuse scattered paths from the walls. For reflected paths from the wall, ground, and ceiling, the material permittivity is considered when computing the reflection loss. In a considered environment, walls are made up of bricks covered with plaster, and the floor is fitted with marble. Afterward, during the postprocessing phase of the ray-tracing simulation data, the influence of the TX and RX antenna radiation patterns is taken into account.

Here, a special case of an indoor environment, i.e., the tee-junction of the corridor is targeted, as these tee-junctions are widely present in universities, office buildings, shopping malls, schools, etc. For simulations, we have considered the tee-junction environment of the UC3M university corridor, and that is shown in Fig. 1(a). We reconstruct the 3D model of the University corridor for use in the ray tracing simulator by accurately modeling the real environment. Fig. 1(b) shows the 3D model of the actual environment with precise and accurate dimensions, which includes the wooden closet and doors. In the simulation environment, as indicated in Fig. 1(b), the TX is located at a distance of 33.6 m from the back wall of corridor number 1 and is placed at a height of 1 m above the floor. However, in corridor number two, a series of 71 RX points distributed over a 7 m distance with 0.1 m separation is considered for simulations, as indicated by the red dots in Fig. 1(b). The height of all RX points is set to 1 m. The shortest and the farthest point-to-point distance between the RX and TX points are 6.7 m and 7.55 m, respectively. The prime focus of this research work is the study of the sub-THz band, i.e., 100 GHz, however, for comparison purposes, the simulations are also conducted at 3.5 GHz from sub-6 GHz band, and 26.5 GHz from the mmWave frequency band. Fig. 2(a) demonstrates a sample output from a ray tracing tool in 2D, depicting the ray paths between the transmitter and a specific receiver point. Whereas, Fig. 2(b-c) provide three three-dimensional view of ray paths from the TX and RX sides, respectively.

In the post-processing phase of RT simulation data, it is assumed that at the TX end, a custom-made horn antenna with a wide half-power beamwidth (HPBW) is used. The azimuth of the TX antenna is fixed, i.e., 90° , and is facing towards the wall of the corridor as shown in Fig. 1(b). The following cases are considered at the RX end:

Single fixed beam: In the first case, the receiver end is equipped with a single beam high-gain horn antenna (Anteral SGH-26-WR10) with narrow HPBW, and the azimuth of the RX antenna is fixed in a certain direction. The antenna radiation patterns of a custom-made horn antenna and SGH-26-WR10 antenna in both vertical and horizontal planes are shown in Fig. 3(a) and Fig. 3(b), respectively, and their general parameters are given in Table 1 [29].

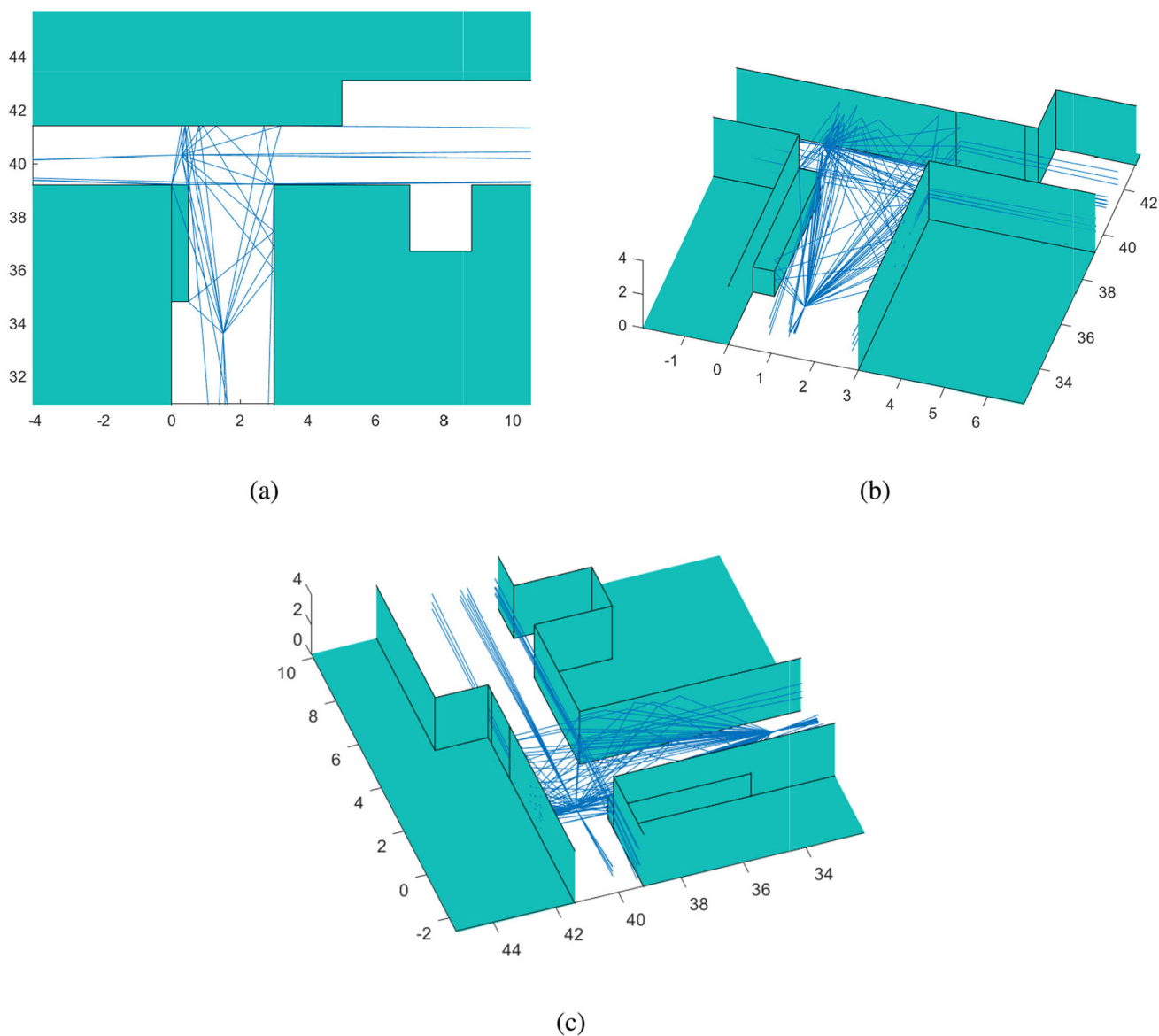


Fig. 2 Illustration of LOS, reflected and diffracted ray paths, (a) 2D view, (b) 3D view from TX side, and (c) 3D view from RX side

Ideal adaptive beam antenna: In this case, a similar antenna is considered at the RX end as in the single fixed beam case; however, it is assumed that the RX antenna has the capability to adjust its beam direction with the granularity of 1° toward the strongest incoming path from the transmitter. In the simulation, the selection of beam direction in the azimuth plane is achieved by rotating the RX antenna 360° with a step size of 1° in the horizontal plane and then selecting the direction that provides the maximum received power at the RX.

Switched beam antenna: In the last case, a switched beam antenna with a different number of fixed beams in the horizontal plane is utilized at the receiver. In this study, we have examined switched beam antennas with 8-, 12-, 18-

, and 24-beams. Sample radiation patterns of switch beam antennas with 8 and 12 beams in the azimuth plane are presented in Fig. 3(c) and Fig. 3(d), respectively. A switched beam antenna with 12 fixed beams exhibits more overlap between the beams compared with 8 fixed beams, and this overlap is further extended with the increase in the number of beams.

It should be noted that the same antenna is used for simulations at 3.5 GHz, 26.5 GHz, and 100 GHz. The transmit power at all considered frequencies is set to 21 dBm.

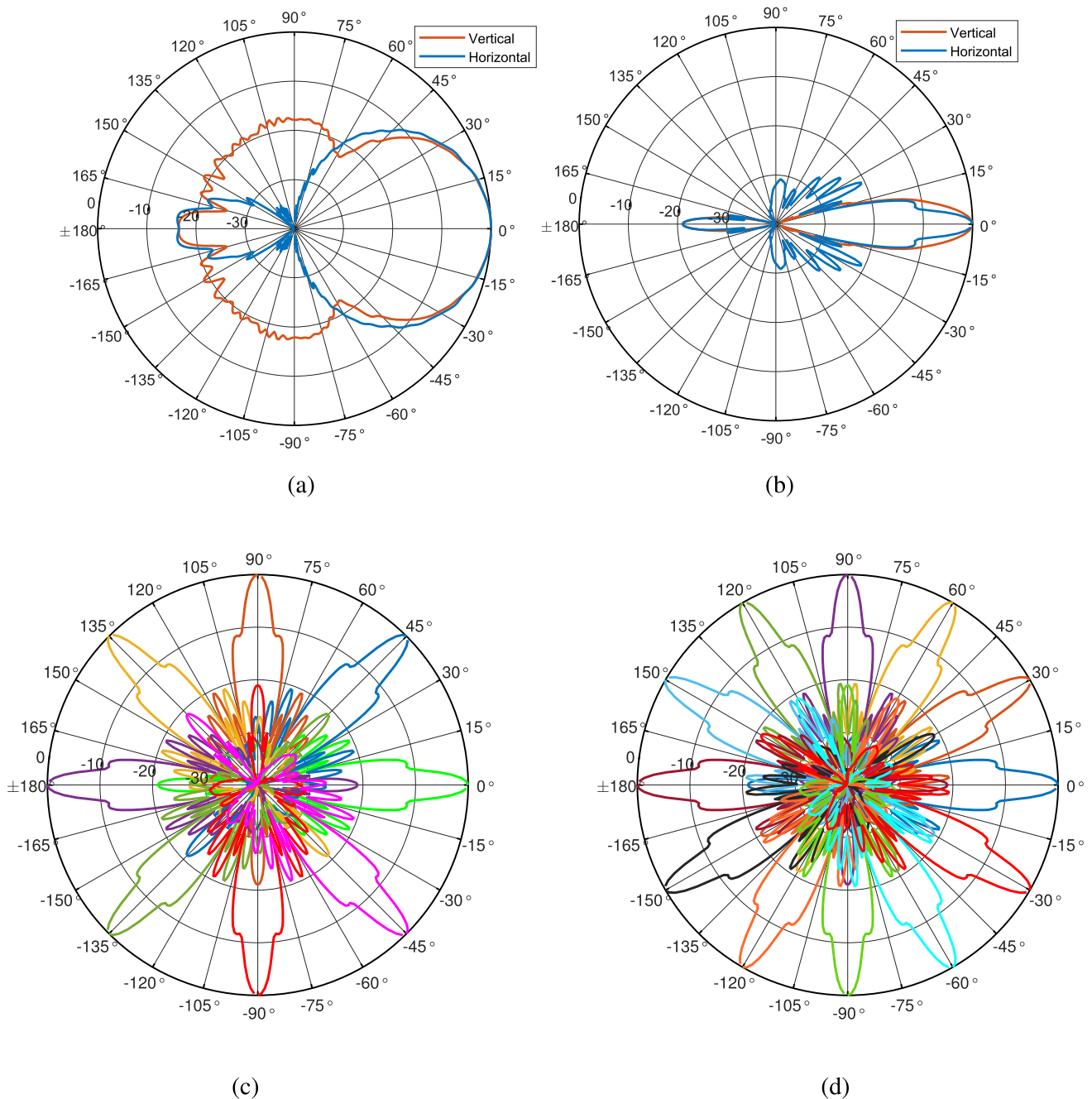


Fig. 3 Radiation pattern of, (a) Single wide beam TX antenna, (b) Single narrow beam RX antenna, (c) Switched beam antenna at RX with 8 beams in horizontal plane, and (d) Switched beam antenna at RX with 12 beams in horizontal plane

4 Results and discussion

The initial phase of the simulations involves the utilization of a single-narrow HPBW antenna at the RX end with fixed azimuth, and afterward, an adaptive antenna at the receiving end is considered. Fig. 4(a) shows the received power along the simulation route at 100 GHz for the RX antenna fixed in four different directions in the azimuth plane, i.e., 0° , 90° , 180° , and 270° . For reference, the received power at all con-

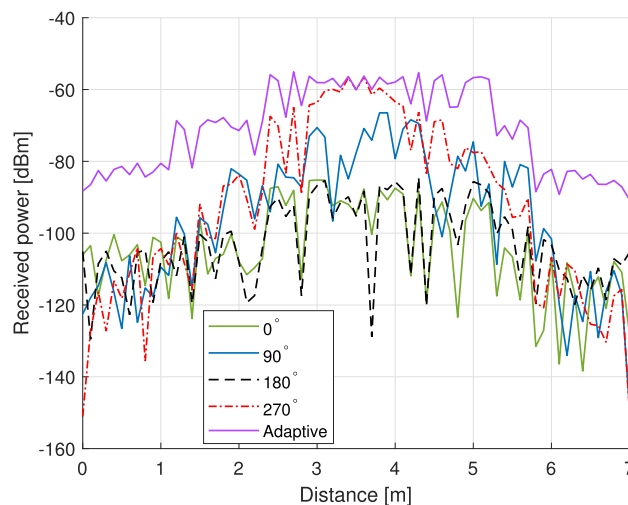
sidered RX points while utilizing a full adaptive antenna with 1° steering capability is also shown in Fig. 4(a). It should be noted that maximum received power is achieved in the middle of the route with the RX antenna pointing towards 270° , as RX was in line with TX and were facing towards each other. Similarly, in the LOS region, the received power with 270° azimuth is clearly higher compared with other fixed antenna cases. However, at RX points located deep within the corridor, the received power with 270° RX antenna was lower

Table 1 General antenna parameters of single beam antennas

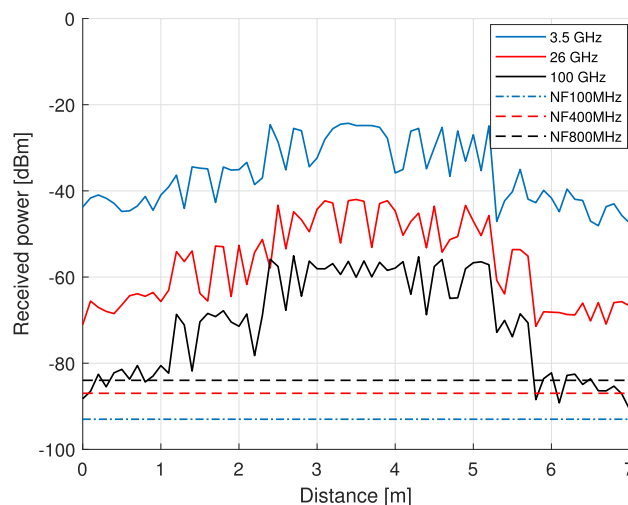
Custom horn antenna			SGH WR-10		
Max gain [dBi]	HPBW Vert [°]	HPBW Horz [°]	Max gain [dBi]	HPBW Vert [°]	HPBW Horz [°]
12.58	45.5	45	27.62	7.7	8.5

among all considered cases. Moreover, the RX antenna with 90° azimuth can capture the strong reflected path from the back wall of corridor one. Conversely, the cases of 0° and 180° exhibit almost similar performance and are certainly not the optimal choices. The results presented in Fig.4(a) clearly indicate that the communication at the sub-THz band with a single fixed beam antenna is a sub-optimal choice as none of the examined cases can provide a satisfactory level of received power across all considered RX points. Whereas, adaptive antenna not only exhibits outstanding performance in the LOS region rather it also delivers significantly better performance in the NLOS region, compared with all fixed antenna cases.

Fig.4(b) shows the received power along the simulation route at the receiver utilizing an adaptive antenna with beam steering along the simulation route, for three different considered frequencies. As expected, the lower frequency of operation provides the higher received power, as path loss is inversely proportional to the frequency. Fig.4(b) explicitly shows that there are three regions present in the simulation route, i.e., line-of-sight (LOS), non-LOS (NLOS) region with reflection, and NLOS region with diffraction. In between the whole simulation route, the RX maintains an LOS connection with the TX in the range from 2.5m to 5.2m. The ray tracing data shows that at least a single reflected path was available for distances between 0m and 2.4m, and 5.3 to 5.8m, and for the rest of the points, other than LOS points, only diffracted ray paths were present. Therefore, a step change in the received power is witnessed while moving from one region to another region of the simulation route. Moreover, it can be noticed that those transitions between the regions are sharper at 26.5 GHz and 100 GHz as compared with 3.5 GHz, and it shows the better radio propagation condition in the NLOS environment at lower frequencies. The mean received power level along the whole simulation route was -36 dBm, -56.5 dBm, and -70.9 dBm, at 3.5 GHz, 26.5 GHz, and 100 GHz, respectively. It illustrates that almost 20 dB power is lost while migrating from 3.5 GHz to 26.5 GHz, followed by an additional 14.5 dB loss while transiting from 26.5 GHz to 100 GHz. It should be noted that here we are dealing with small distances only, and the maximum point-to-point distance considered in the simulation is just 7.55m. Even at such short distances in an NLOS environment, the received power level is diminished to approximately -89 dBm while employing adaptive



(a)

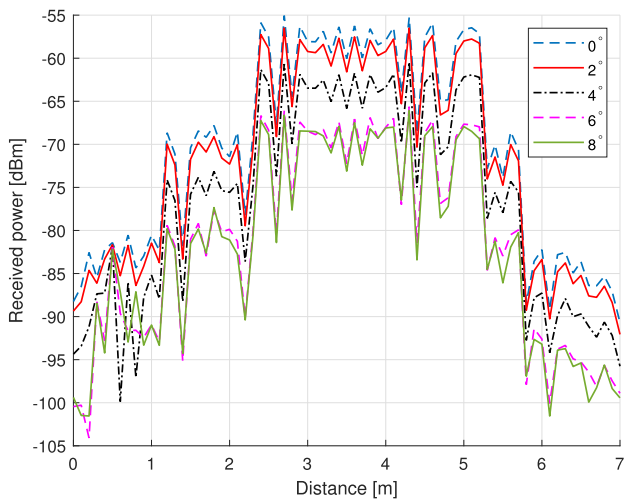


(b)

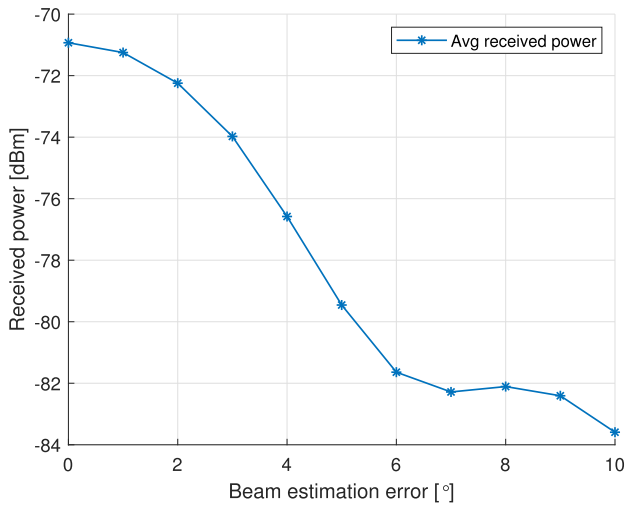
Fig. 4 Received power along the simulation route, (a) At 100 GHz with fixed and ideal adaptive beam antenna at the receiver end, and (b) At different frequencies with ideal adaptive beam antenna at RX

beam steering, whereas the noise floor at room temperature with 100, 400, 800 MHz bandwidth is -93.87, -87.96, and -84.95 dBm, respectively. The receiver noise floor with 100, 400, 800 MHz bandwidth is highlighted in Fig.4(b). These results indicate that the communication at the sub-THz band, i.e., 100 GHz is quite challenging under the NLOS condition. Here, it is important to highlight that for comparison purposes we have utilized the same antenna pattern for the three considered frequencies. However, to have the same antenna pattern, the size of the antenna would be different, i.e., much larger at lower frequencies. Therefore, the received power at 3.5 GHz and 26.5 GHz can be scaled down with respect to the maximum antenna gain at the considered frequencies.

So far, an antenna capable of steering its beam with zero estimation error, i.e., the ideal case, is considered at the receiver. However, in reality, multiple factors may lead to



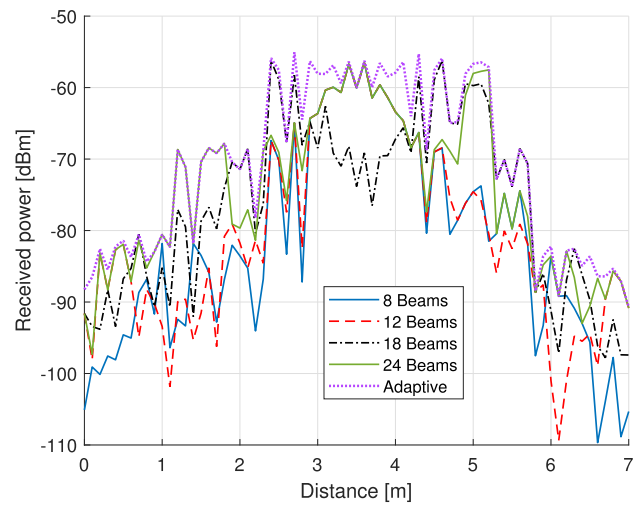
(a)



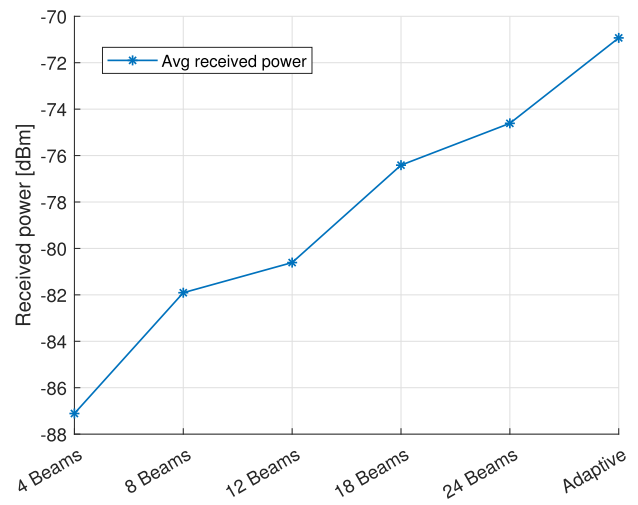
(b)

Fig. 5 Received power at 100 GHz with full adaptive antenna, (a) Along the simulation route with different beam estimation error, and (b) Mean received across all RX points with different beam estimation error

erroneous beam estimation. Therefore, it is interesting to evaluate the impact of beam estimation error, or in other words, beam-pointing error, on the received power level at the RX. Fig. 5(a) and Fig. 5(b) show the received power and the mean received power along the simulation route, respectively, at an operating frequency of 100 GHz while considering different beam estimation error. It is critical to mention here that a fixed error of 0°, 2°, 4°, 6°, and 8° is taken into account for the analysis, where 0° is the reference case and represents an ideal adaptive beam steering scenario. It can be seen in Fig. 5(a) that considering an RX antenna with 8.5° HPBW in the horizontal plane, there is no significant change observed in the received power level with up to 2° of beam estimation error. However, the results presented in Fig. 5(b) show that the mean received power level



(a)



(b)

Fig. 6 Received power at 100 GHz with while utilizing SBAs with different number of fixed switch beams (a) Across all RX points, and (b) Mean received power of the simulation route

is significantly impacted with 3° of beam estimation error, and the sharp reduction in received power continues up to 6° of BEE. The mean received power exhibits a decrease of almost 3 dB, 5.6 dB, and 10.7 dB at beam estimation errors of 3°, 4°, and 6°, respectively, compared with the reference case. It shows that an accurate beam estimation is required for beam steering to avoid the loss of signal strength, whereas a small BEE of 4° is already causing significant damage, i.e., 5.6 dB, to the received signal strength. These results highlight the fact that proper antenna alignment with minimum beam estimation error correction is crucial to mitigate the problem of reduced RX power and ensure reliable signal reception.

Fig. 6(a) shows the received power across all receiving points at a sub-THz frequency of 100 GHz for switched beam antennas with different numbers of beams, i.e., 8, 12, 18, and

24. It is already shown in Fig. 3(c-d) that the beam overlapping in the azimuth plane extends with the increase in the number of beams. Consequently, it was natural to anticipate an enhancement in received signal power at all points with the increasing number of beams. However, the results depicted in Fig. 6(a) contradict this expectation. It should be noted that in Fig. 6(a), for the distance between 3-4m, there is an overlap between the graph line of 24-beams SBA and the graph lines of 8-, and 12-beams SBAs. In contrast, the 18-beams antenna case exhibits a distinct value during this range. It points out a critical aspect of SBA that for 8-, 12-, and 24-beams SBAs, the beams are pointing at the multiples of 15° in the azimuth plane, while in the case of 18-beams SBA, the beams are pointing at the multiples of 20° . It is important to mention here that in our simulations, beam number 1 is always set in the zero direction in the azimuth plane, and therefore, 18-beams SBA has different behavior compared with other cases. Results presented in Fig. 6(a) highlight the fact that in the case of SBA, the beam directions should be properly aligned with respect to the target spots to be covered, and it depicts a downside of SBA. It is clearly evident that a fully adaptive antenna with a steering accuracy of 1° outperforms all cases of SBAs in terms of received power level. Finally, Fig. 6(b) shows the mean received power with different SBAs, considering all RX points for simulations. Now, it is interesting to make a comparison between SBAs employing different numbers of beams and a fully adaptive antenna operating with different levels of beam pointing error. The analysis of the results presented in Fig. 5(b) and Fig. 6(b) reveals that the mean received power levels of around -74.6 dBm and -76.4 dBm are achieved with the use of 24-beams and 18-beams SBAs, respectively. These values closely align with the received power levels of -74.0 dBm and -76.6 dBm attained through the utilization of a fully adaptive antenna with beam estimation errors of 3° and 4° , respectively. In a real-world scenario, maintaining a low level of beam estimation error can be quite challenging, and the process of beam steering itself demands significant computational resources. Conversely, SBAs offer a simpler implementation, and the findings presented in this paper indicate that with a sufficiently high number of beams, SBAs can deliver almost equivalent levels of performance in terms of received power as a fully adaptive antenna with low beam estimation error.

5 Conclusions

The main target of this study was to analyze the impact of different antenna solutions, i.e., utilization of a single fixed-beam antenna, a fully adaptive antenna, and a switched beam antenna at the receiver, for an indoor wireless network operating at a sub-THz frequency band. We focused

on a common tee-junction location within a building corridor and conducted ray tracing simulations for a series of RX points, encompassing both LOS and NLOS scenarios with the transmitter. A calibrated and validated in-house built ray tracing tool was used for conducting ray tracing simulations. The obtained results clearly indicate that for a receiver with mobility, the utilization of a fixed single-beam antenna at the RX end is the least preferred choice among the considered antenna solutions. An ideal adaptive antenna with 0° beam pointing error exhibits outstanding performance in both the LOS and NLOS regions. It is found that there is a reduction of approximately 20 dB in a received power level while changing the frequency of operation from 3.5 GHz to 26.5 GHz, followed by an additional 14.5 dB loss when transiting from 26.5 GHz to 100 GHz. The beam pointing error is a common issue in active adaptive antennas. Considering an adaptive RX antenna with 8.5° HPBW in an azimuth plane, interestingly, it was found that there is no significant reduction in the received power level with up to 2° of the beam estimation error. Whereas, the mean received power at 100 GHz is decreased by almost 3 dB, 5.6 dB, and 10.7 dB with beam estimation errors of 3° , 4° , and 6° , respectively, compared with the 0° reference case. Switch beam antennas are less complex, easy to implement, and have less overhead compared to adaptive beam steering antennas. The obtained results indicate that the gain of SBA depends on the number of switched beams, and almost similar mean received power levels were achieved with 24 and 18 SBA beams as those achieved with a fully adaptive antenna with 3° , 4° beam estimation error. Moreover, results presented in the article also highlighted one crucial aspect of SBA, that in the case of SBA, the beam directions are set and fixed, and they may fail to align with the target spot if not adjusted properly.

Author Contributions Here is a list of authors with their initials: Muhammad Usman Sheikh (M.U.S) Kalle Ruttik (K.R) Riku Jantti (R.J) Jyri Hamalainen (J.H) M.U.S, K.R, R.J were mainly involved in the conceptual framework of this research work. M.U.S is responsible for simulations and data collection. M.U.S is responsible for performing statistical data analysis, and figure creations. M.U.S, K.R, R.J, J.H are involved in detailed result analysis, in collecting insights, and in collecting main outcomes of this research work. M.U.S initiated the writing of main draft. M.U.S, K.R, R.J, J.H were involved in editing and reviewing the manuscript. M.U.S, K.R, R.J, J.H were involved in proofreading of the manuscript. R.J was supervising this project. R.J was responsible for securing funding for this project.

Funding Open Access funding provided by Aalto University. This work has been partially supported by Business Finland project 6G-EXP.

Data Availability Research data can be made available on request.

Declarations

Competing interests The authors declare no competing interests.

Open Access This article is licensed under a Creative Commons Attribution 4.0 International License, which permits use, sharing, adaptation, distribution and reproduction in any medium or format, as long as you give appropriate credit to the original author(s) and the source, provide a link to the Creative Commons licence, and indicate if changes were made. The images or other third party material in this article are included in the article's Creative Commons licence, unless indicated otherwise in a credit line to the material. If material is not included in the article's Creative Commons licence and your intended use is not permitted by statutory regulation or exceeds the permitted use, you will need to obtain permission directly from the copyright holder. To view a copy of this licence, visit <http://creativecommons.org/licenses/by/4.0/>.

References

- Lyu, Y., Kyösti, P. & Fan, W. (2021). Sub-thz vna-based channel sounder structure and channel measurements at 100 and 300 ghz, In *2021 IEEE 32nd Annual International Symposium on Personal, Indoor and Mobile Radio Communications (PIMRC)* (pp. 1–5).
- Puerta, R. & Queseth, O. (2022). Sub-terahertz performance for beyond 5g in indoor environments, In *ICC 2022 - IEEE International Conference on Communications* (pp. 3766–3771).
- Abbasi, N. A., Hariharan, A., Nair, A. M., Almainan, A. S., Rotenberg, F. B., Willner, A. E., & Molisch, A. F. (2020). Double directional channel measurements for thz communications in an urban environment, In *ICC 2020 - 2020 IEEE International Conference on Communications (ICC)* (pp. 1–6).
- Trzebiatowski, K., Rzymowski, M., Kulas, L., & Nyka, K. (2021). Simple 60 ghz switched beam antenna for 5g millimeter-wave applications. *IEEE Antennas and Wireless Propagation Letters*, 20(1), 38–42.
- Roh, W., Seol, J.-Y., Park, J., Lee, B., Lee, J., Kim, Y., Cho, J., Cheun, K., & Aryanfar, F. (2014). Millimeter-wave beamforming as an enabling technology for 5g cellular communications: Theoretical feasibility and prototype results. *IEEE Communications Magazine*, 52(2), 106–113.
- Yang, C.-F., Wu, B.-C., & Ko, C.-J. (1998). A ray-tracing method for modeling indoor wave propagation and penetration. *IEEE Transactions on Antennas and Propagation*, 46(6), 907–919.
- Soni, S., & Bhattacharya, A. (2012). An efficient two-dimensional ray-tracing algorithm for modeling of urban microcellular environments. *International Journal of Electronics and Communications*, 66(6), 439–447.
- Lotti, M., Caillet, M., & D'Errico, R., (2022). Comparison of indoor channel characteristics for sub-thz bands from 125 ghz to 300 ghz, In *2022 16th European Conference on Antennas and Propagation (EuCAP)* (pp. 1–5).
- Moon, S.-R., Kim, E.-S., Sung, M., Rha, H. Y., Lee, E. S., Lee, I.-M., Park, K. H., Lee, J. K., & Cho, S.-H. (2022). 6g indoor network enabled by photonics- and electronics-based sub-thz technology. *Journal of Lightwave Technology*, 40(2), 499–510.
- Xing, Y., Rappaport, T. S., & Ghosh, A. (2021). Millimeter wave and sub-thz indoor radio propagation channel measurements, models, and comparisons in an office environment. *IEEE Communications Letters*, 25(10), 3151–3155.
- Ju, S., Xing, Y., Kanhere, O. & Rappaport, T. S. (2022). Sub-terahertz channel measurements and characterization in a factory building, In *ICC 2022 - IEEE International Conference on Communications* (pp. 2882–2887).
- Sheikh, M. U., Ali, M., Carpintero, G., Ruttik, K., Mutafangwa, E., & Jäntti, R. (2022). Power angular measurements and ray tracing simulations at sub-thz frequencies in corridor, In *2022 IEEE Wireless Communications and Networking Conference (WCNC)* (pp. 1587–1592).
- Sheikh, M. U., Ali, M., Carpintero, G., Ruttik, K., Mutafangwa, E., & Jäntti, R. (2023). Channel characterization at sub-thz band with measurements and ray tracing in indoor case, In *2023 International Conference on Information Networking (ICOIN)* (pp. 178–183).
- Katare, K. K., Chandravanshi, S., Biswas, A., & Akhtar, M. J. (2018). Beam steering architectures for next-generation cellular wireless applications, In *2018 IEEE MTT-S International Microwave and RF Conference (IMaRC)* (pp. 1–3).
- Ullah, M. S., & Tewfik, A. (2018). Beam detection analysis for 5g mmwave initial acquisition, In *2018 28th International Telecommunication Networks and Applications Conference (ITNAC)* (pp. 1–8).
- Dadgarpour, A., Zarghooni, B., Virdee, B. S., & Denidni, T. A. (2016). One- and two-dimensional beam-switching antenna for millimeter-wave mimo applications. *IEEE Transactions on Antennas and Propagation*, 64(2), 564–573.
- Tao, S., Zhao, H., Ban, Y.-L., & Chen, Z. (2020). An overlapped switched-beam antenna array with omnidirectional coverage for 2.4/5.8 ghz three-channel mimo wlan applications. *IEEE Antennas and Wireless Propagation Letters*, 19(1), 79–83.
- Ghani, F. A., Uzun, A., Saleh, H. A., Yapici, M. K., & Tekin, I. (2020). A 28 ghz 2 × 2 antenna array with 10 beams using passive beamforming network, In *2020 IEEE International Symposium on Antennas and Propagation and North American Radio Science Meeting* (pp. 1747–1748).
- Patterson, C. E., Khan, W. T., Ponchak, G. E., May, G. S., & Pappalopolymerou, J. (2012). A 60-ghz active receiving switched-beam antenna array with integrated butler matrix and gaas amplifiers. *IEEE Transactions on Microwave Theory and Techniques*, 60(11), 3599–3607.
- Tseng, C.-H., Chen, C.-J., & Chu, T.-H. (2008). A low-cost 60-ghz switched-beam patch antenna array with butler matrix network. *IEEE Antennas and Wireless Propagation Letters*, 7, 432–435.
- Nazneen, Z., Sunder, M. S., Bharath, K., & Ramakrishna, D. (2019). 4-stage switched beam phased array antenna using butler matrix, In *2019 IEEE Indian Conference on Antennas and Propagation (InCAP)* (pp. 1–4).
- Moknache, A., Dussopt, L., Säily, J., Lamminen, A., Kaunisto, M., Aurinsalo, J., Bateman, T., & Francey, J. (2016). A switched-beam linearly-polarized transmitarray antenna for v-band backhaul applications, In *2016 10th European Conference on Antennas and Propagation (EuCAP)* (pp. 1–5).
- Tang, C. -L. & Chen, C. -H. (2016). Switched-beam antenna for small cell application, In *2016 International Symposium on Antennas and Propagation (ISAP)* (pp. 100–101).
- Li, Y. & Hao, Z. -C. (2017). A wideband switched beam antenna for full 360 coverage, In *2017 Sixth Asia-Pacific Conference on Antennas and Propagation (APCAP)* (pp. 1–3).
- Yun, Z., & Iskander, M. F. (2015). Ray tracing for radio propagation modeling: Principles and applications. *IEEE Access*, 3, 1089–1100.
- Ling, H., Chou, R.-C., & Lee, S.-W. (1989). Shooting and bouncing rays: Calculating the rcs of an arbitrarily shaped cavity. *IEEE Transactions on Antennas and Propagation*, 37(2), 194–205.
- Durgin, G., Patwari, N., & Rappaport, T. (1997). Improved 3d ray launching method for wireless propagation prediction. *Electronics Letters*, 33(16), 1412–1413.
- Tan, S., & Tan, H. (1996). A microcellular communications propagation model based on the uniform theory of diffraction and multiple image theory. *IEEE Transactions on Antennas and Propagation*, 44(10), 1317–1326.
- [Online]. Available: <https://antenal.com/datasheets/standard-gain-horn-antenna-wr10-26-dbi-gain.pdf>.

Publisher's Note Springer Nature remains neutral with regard to jurisdictional claims in published maps and institutional affiliations.

Kalle Ruttik received the Diploma degree in engineering from Tallinn Technical University, in 1993, and the Lic.Tech. degree from the Helsinki University of Technology, in 1999. He received his D.Sc. (Tech.) degree in Telecommunications Technology from Aalto University in 2011. He is currently a Teaching Researcher with the Department of Communications and Networking (ComNet), School of Electrical Engineering, Aalto University. His research interests include radio physical layer algorithms, software radio, and cloud RAN.

Riku Jäntti is a Full Professor of Communications Engineering at Aalto University School of Electrical Engineering, Finland. He received his M.Sc (with distinction) in Electrical Engineering in 1997 and D.Sc (with distinction) in Automation and Systems Technology in 2001, both from Helsinki University of Technology (TKK). Prior to joining Aalto (formerly known as TKK) in August 2006, he was professor pro tem at the Department of Computer Science, University of Vaasa. Prof. Jäntti is a senior member of IEEE. He was also IEEE VTS Distinguished Lecturer (Class 2016). The research interests of Prof. Jäntti include low-power wireless systems, machine type communications, Cloud based Radio Access Networks, spectrum and co-existence management, quantum communications and RF Inference.

Jyri Hamalainen is Full Professor and currently working as Vice President, Research Services of Aalto University, Finland. He received his M.Sc. and Ph.D. degrees from University of Oulu, in 1992 and 1998, respectively. From 1999 until the end of 2007 he was a Senior Specialist and Program Manager in Nokia where he worked with various aspects of mobile communication systems and 3GPP standardization. Hämäläinen was nominated to professor of Aalto University in 2008 and he was tenured in 2013. His research interests cover mobile and wireless systems, special focus being in irregular, dynamic and heterogeneous networks including e.g. 5G, small cells, multi-antenna transmission and reception techniques, scheduling, relays and many other topics. Hämäläinen is author or co-author of over 200 scientific publications and 37 US patents or patent applications. He is a Senior Member of IEEE and an Expert Member of the Highest Administrative Court of Finland, nominated by the President of Finland.

Muhammad Usman Sheikh born in Rawalpindi, Pakistan, in 1983. He received his B.Sc. degree in Electrical Engineering from CIIT Islamabad, Pakistan in 2006. He received his M.Sc. and D.Sc. (Tech) degrees from Tampere University of Technology (TUT), Finland in 2009 and 2014, respectively. Currently, he is working as a Performance Specialist at NOKIA and working as part-time post-doctoral researcher at Aalto University, Finland. He has more than 15 years of experience from different radio network planning and optimization projects. His general interests include network planning and optimization, future mobile technologies, radio propagations, channel modeling, 3D ray tracing, advanced antennas and novel and innovative cellular concepts. He is the author of several international journal articles, conference papers, and book chapters and he is a senior IEEE member.